Combining the correlation-stability approach to OCT elastography with the speckle-variance evaluation for quantifying the stiffness differences

Lev A. Matveev[1,2,3]*, Vladimir Yu. Zaitsev[1,2,3], Alexandr L. Matveyev[1,2], Grigory V. Gelikonov[1,2], Valentin M. Gelikonov[1,2,3]
[1]Institute of Applied Physics Russian Academy of Sciences, Ulyanova Street 46, 603950 Nizhniy Novgorod, Russia
[2]Nizhny Novgorod State Medical Academy, Minin Square 10/1, 603005 Nizhny Novgorod, Russia
[3]Nizhny Novgorod State University, Gagarina Avenue 23, Nizhny Novgorod 603950, Russia

ABSTRACT

We discuss an advanced variant of the correlation-stability (CS) approach to OCT elastography that is capable of quantifying the stiffness differences. The modified variant is based on natural combination of CS approach with the speckle-variance (SV) approach. It allows one to determine the strain dependence of the normalized speckle intensity variance function for two compared subsets taken from the OCT images corresponding to the initial and deformed states of the tissue. In previous studies we considered the basic dependence of the normalized speckle intensity variance function on the tissue strain under the assumption that the influence of translational displacements can be excluded, so that the residual speckle-intensity variations should be produced only by speckle blinking determined by local strains. In the present report we discuss the corresponding algorithms allowing one to exclude the above-mentioned influence of translational displacements. We demonstrate numerically the efficiency of such processing that allows for quantification of stiffness differences in the elastographic mapping based on the CS approach.

Keywords: optical coherence tomography, elastography, image processing, correlation-stability approach, speckle variance, digital image correlation

1. INTRODUCTION

The possibilities of elastographic mapping based on processing OCT images of quasistatically deformed biological tissues have attracted significant attention during the last 15 years[1] (on the latest achievements see, e.g., reviews[2,3]). However, until now elastographic methods have not yet been implemented in OCT scanners intended for practical medical applications. The main reason of such a situation is due to the fact of unexpectedly difficult implementation of the apparently simple idea of the use of quasistatic straining of the tissue: standard realizations of such compression-using approaches require sufficiently accurate reconstruction the displacement field in the examined tissue region[1-5]. Then a rather error-sensitive procedure of numerical differentiation of the displacements should be performed in order to reconstruct local strains and thus evaluate the differences in the local stiffness of the tissue. Independently of the particular methods for measuring displacements (e.g., digital image or volume correlation[6-11] or phase-resolved[12-19]), all such approaches are displacement-based ones. Phase-sensitive optical coherence tomography provides the possibility to measure the elastic wave propagation using very high speed full-field OCT systems[20-22]. But for the common OCT systems with frame rate 10 - 40 B-scans per second such phase-sensitive methods are not practically feasible. For common OCT devices more robust approaches to OCT elastography are needed. To avoid the error-sensitive two-stage procedure of visualization of the stiffness-difference, recently an alternative, the so-called correlation-stability (CS) approach was proposed[23-26]. It is based on the idea that decrease in the cross-correlation between the corresponding fragments of the compared images is determined by the degree of the mutual displacements of the scatterers belonging to the compared image fragments. The degree of these mutual displacements of the scatterers is in turn determined by the local strains. Like in the above-mentioned displacement-based approaches, the elastic stress in the examined region is

*lionnn52rus@mail.ru; phone 7 831 436-7293; fax 7 831 436-5976; iapras.ru

Biophotonics: Photonic Solutions for Better Health Care IV, edited by Jürgen Popp, Valery V. Tuchin, Dennis L. Matthews, Francesco S. Pavone, Proc. of SPIE Vol. 9129, 91290I · © 2014 SPIE · CCC code: 0277-786X/14/$18 · doi: 10.1117/12.2052144

supposed to be fairly uniform, which is reasonable in the vicinity of the strain-producing OCT probe. In the simplest variants[23-26], the CS approach can be used for qualitative elasticity mapping. In general it is close to correlation mapping OCT utilized for micro-vasculature visualization, where the speckle decorrelation is produced by the Brownian motion of scatterers in liquids[27,28]. In our previous work[29] we considered an advanced variant of the CS approach that is capable of quantifying the stiffness differences. Using the general similarity with the speckle-variance due to the Brownian motion in the micro-vasculature visualization[30-36] and the strain-produced motion in elastographic problems, we modify the CS approach to determine the dependence of speckle intensity variance function on strain[29].

In the general case, speckle intensity variation can be produced by both the translational displacements (related to speckle translation and therefore flux of the intensity form one pixel to another with total luminance energy conservation)[37-38], as well as by local strains (related to speckle blinking without any intensity flux from one pixel to another)[29,37-38]. As it was shown in our previous study[29] the normalized speckle intensity variation function (NSIVF) for two subsets taken from the tissue images in the initial and deformed states is given by:

$$V = \frac{Var(\left|\widetilde{S}\right| - \left|\widetilde{F}_{n^*,k^*}\right|)}{\sqrt{Var(\widetilde{S}) \cdot Var(\widetilde{F}_{n^*,k^*})}}, \tag{1}$$

where:

$$\begin{cases} Var(\left|\widetilde{S}\right| - \left|\widetilde{F}_{n^*,k^*}\right|) = \dfrac{1}{m_1 m_2} \sum_{i=1}^{m_1} \sum_{j=1}^{m_2} (\left|\widetilde{S}_{i,j}\right| - \left|\widetilde{F}_{i+n^*,j+k^*}\right|)^2 \\ Var(\widetilde{S}) = \dfrac{1}{m_1 m_2} \sum_{i=1}^{m_1} \sum_{j=1}^{m_2} \widetilde{S}_{i,j} \cdot \widetilde{S}^*_{i,j} \\ Var(\widetilde{F}_{n^*,k^*}) = \dfrac{1}{m_1 m_2} \sum_{i=1}^{m_1} \sum_{j=1}^{m_2} \widetilde{F}_{i+n^*,j+k^*} \cdot \widetilde{F}^*_{i+n^*,j+k^*} \end{cases}, \tag{2}$$

and $\widetilde{S}$ and $\widetilde{F}_{n^*,k^*}$ are the subsets (with a full-field OCT signal recorded as complex number for each pixel) $m_1 \times m_2$ in size taken from the initial and deformed images with their average values subtracted, $\widetilde{S} = S - \mu_s$ and $\widetilde{F}_{n^*,k^*} = F_{n^*,k^*} - \mu_{F_{n^*,k^*}}$, the quantities ($n^*$,$k^*$) correspond to the vector of translational displacement of the subset $\widetilde{F}_{n^*,k^*}$ with respect to $\widetilde{S}$. Here $\widetilde{S}^*$ and $\widetilde{F}^*_{n^*,k^*}$ are the complex conjugate of $\widetilde{S}$ and $\widetilde{F}_{n^*,k^*}$. Zero-mean normalized cross-correlation function (ZMNCCF):

$$C(n^*,k^*) = \frac{\dfrac{1}{m_1 m_2} \sum_{i=1}^{m_1} \sum_{j=1}^{m_2} (\widetilde{S}_{i,j} \cdot \widetilde{F}^*_{i+n^*,j+k^*})}{\sqrt{Var(\widetilde{S}) \cdot Var(\widetilde{F}_{n^*,k^*})}}, \tag{3}$$

is related with NSIVF (1) as[29]:

$$V = \frac{Var(\left|\widetilde{S}\right| - \left|\widetilde{F}_{n^*,k^*}\right|)}{\sqrt{Var(\widetilde{S}) \cdot Var(\widetilde{F}_{n^*,k^*})}} = \frac{Var(\widetilde{S}) + Var(\widetilde{F}_{n^*,k^*})}{\sqrt{Var(\widetilde{S}) \cdot Var(\widetilde{F}_{n^*,k^*})}} - 2 \cdot \left|C(n^*,k^*)\right|, \tag{4}$$

and NSIVF is related to the strain ε as $V \propto \varepsilon^2$ (see our previous study[29] and upcoming publications). Thus the square root of V is a linear function of strain. This means that for the local strains $\varepsilon_{1,2}$ determined by the elastic moduli $E_{1,2}$ of two different regions of the tissue subjected to the same stress in the vicinity of the OCT probe the following relation is valid[29]:

$$\frac{\sqrt{V_{region1}}}{\sqrt{V_{region2}}} = \frac{\varepsilon_1}{\varepsilon_2} = \frac{E_1}{E_2}. \tag{5}$$

Thus speckle-variance ratio (5) gives the ratio of the local strains and, therefore, the ratio of the local stiffness values[29] when the contributions of translational displacements (including those accumulated at different depths due to the applied strain) are excluded. In the next section we will discuss the preprocessing of full-field OCT (FF-OCT) images that can ensure compensation of the translational displacements. Its efficiently will be illustrated by numerical simulations.

2. EXCLUDING THE CONTRIBUTION OF TRANSLATIONAL DISPLACEMETNS FROM THE SPECKLE VARIANCE FUNCTION BY PREPROCESSING OCT IMAGES AND NUMERICAL DEMONSTRATIONS OF THE METHOD

For correct quantification of stiffness contrast using the speckle variance modification of the CS approach, the key issue is the elimination of contribution given by translational shifts and displacements of the scatterers in the OCT image of the deformed tissue, so that only the contribution of speckle-blinking (determined by local stains) remains in the calculated NSIVF. Translational displacements can be divided into "large" and "small" ones. Large displacements are the displacements on the scale of several integer pixels. Such displacements can be determined using basic cross-correlation processing with a precision of ± 0.5 pixels. Under small displacements we understand the displacements of the sub-pixel scale. The compensation of both large (integer number of pixels) and small (sub-pixel) scales of the actual displacement is important and should be performed for each individual subset $\widetilde{F}_{n^*,k^*}$, because the displacement field induced by tissue straining is different in different regions (e.g. for different depths) within the processed OCT image. After straightforward compensation of large (integer-pixel) displacements using standard digital image correlation processing, it is necessary to compensate the residual small sub-pixel displacements for each subset taken from the deformed image. To compensate these remaining sub-pixel displacements, we apply the processing of full-field (complex) OCT signal in the spectral domain. The method is based on precise localization of maxima of the absolute value of the complex cross-correlation function for the deformed and reference images by applying small (within ± 0.5 pixel) relative displacements of the compared subsets. Because of discrete nature of the OCT images in the space domain, we use the FFT transform of the considered subset into spectral domain. Using the theorem about the spectrum of functions with shifted arguments, we apply multiplication of the Fourier-components by the appropriate complex exponential factor in order to obtain the spectrum corresponding to the subset shifted by any desired sub-pixel value in the space domain. Then performing the inverse transform, the spatial form of the shifted subset can be obtained and used for calculation of cross-correlation with the reference subset. Maximization of the cross-correlation between the reference and so-shifted subset from the deformed image makes it possible to estimate the displacement of this image fragment with the desired sub-pixel accuracy and does not require any special assumptions about the form of the cross-correlation function. As a result of such processing the two images can be superposed with the desired sub-pixel accuracy. After performing such operations, the sought quantity NSIVF given by Eq. (1) for each subset $\widetilde{F}_{n^*\pm\Delta n,k^*\pm\Delta k}$ from the deformed frame and the subset $\widetilde{S}$ from the reference image can be found. The so-calculated value of NSIVF is determined only by speckle blinking induced by local strains, whereas the contribution of the translational displacements is excluded. Insufficient compensation of the subpixel relative displacements of the subsets leads to significant errors in the strain estimation based of the speckle variance approach.

We have numerically simulated two OCT images of a three-layer tissue sample. In this simulation the stiffness contrast of middle layer is 4 times relatively to the surrounding softer tissue. The first simulated frame is the reference frame and the second simulated frame is obtained by simulating the tissue straining with 3% mean strain by applying the above-described procedures. In this simulation we put 10024 randomly distributed independent scatterers in each A-scan which has 256 pixels in depth. The ratio of the coherence length to wave length in this simulation is $L_c / \lambda = 2$, so that the speckle blinking is not so strong as for $L_c / \lambda >> 1$, but still fairly noticeable. To visualize and quantify the stiffness contrast, we apply the proposed speckle-variance modification of the correlation-stability approach. For the plots (a) and (b) in Figure 1, we compensate only large strain-induced displacements, whereas the above-described sub-pixel compensation is not performed. It is seen from Figure 1 that in the plots (a) and (b) the stiffer layer in the middle part of

the image is hardly visible and any quantification is impossible. The non-compensated sub-pixel displacements lead to huge errors.

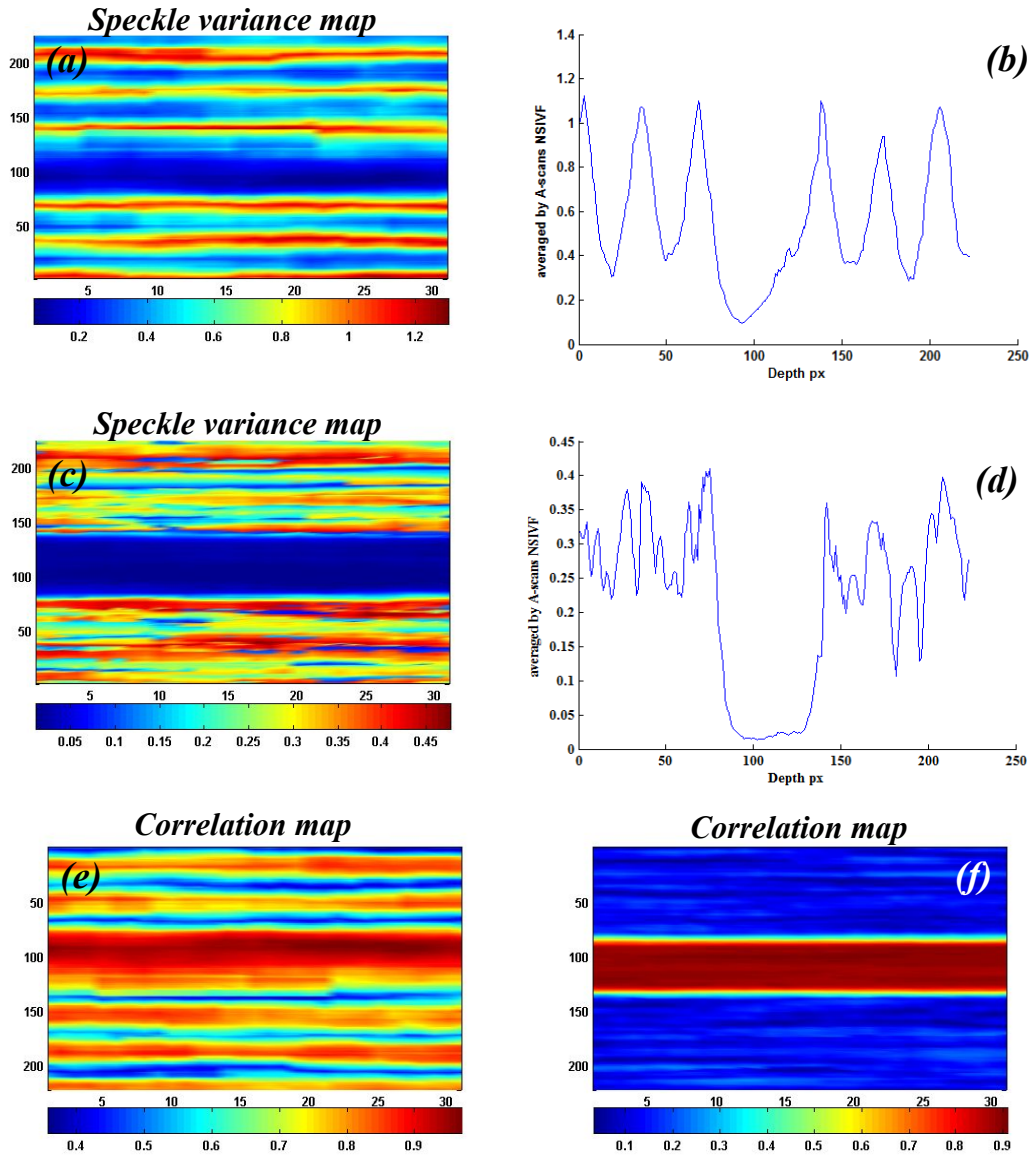

Figure 1. Panel (a) - speckle variance map in the case of large displacement compensation, but without compensation of small sub-pixel displacements. Panel (b) - averaged normalized speckle intensity variance function (NSIVF) averaged over 32 A-scans from panel (a). Panel (c) - speckle variance map obtained if both large and small displacements are compensated using the full-field OCT signal; panel (b) is the corresponding NSIVF averaged over 32 A-scans in such a case. It is clearly seen that the rigid layer is visualized via pronouncedly reduced speckle-variation and the contrast in NSIVF is 15.24, which according to Eq. (5) agrees within the 10% accuracy with the 4 times stiffness contrast used in the simulation of the speckle-pattern distortion. Panels (e) and (f) demonstrate the importance of small subpixel displacement compensations for the improvement of visualization using the correlation-stability approach. Panel (e) is fro the map obtained without compensation of sub-pixel displacemetns and panel (f) is found using the compensation of sub-pixel displacements.

For the plots (c) and (d) in Figure 1, we compensate both large and small sub-pixel displacements using the full complex signal as described above. It is clearly seen that now the layer is much better visualized and the main new advantage of such visualization is that the possibility to quantify the contrast in stiffnesses using the averaged NSIVF for the layer and

the surroundings tissue. The corresponding difference is 15.24 times (averaged NSIVF within the layer is 0.0198 and for the surroundings media it equals to 0.3017). This means[29] that the square root of this value gives us a value rather close (with an error ~0.1) to the 4 times contrast used in the simulation of the speckle-pattern deformation.

The last two plots (e) and (f) in Figure 1 demonstrate how the compensation of small sub-pixel displacements helps to improve the standard[23-26,38] correlation-stability elastograms. Figure 1(e) shows that the groups of scatterers, for which the sub-pixel displacements close to 0.5 pixel are not appropriately compensated, produce artifact lines on the correlation map. After pre-proceeding of complex OCT signal those artifacts are eliminated via appropriate compensation of the small subpixel displacements.

In conclusion we emphasize that the described compensation of small sub-pixel displacements is of key importance for both qualitative visualization and quantification of stiffness contrasts. The critically important feature of this compensation is that the process is based on the full-field OCT signal that allows one to retain only the speckle variance related to local strains and exclude the masking variations related to translational motion (including the accumulated strain-induced depth-dependent translations). Utilization of the complex full-field OCT signal gives the opportunity to correctly compensate the sub-pixel translations and retain only strain-induced speckle-blinking contribution into the normalized speckle intensity variance function.

3. ACKNOWLEDGEMENTS

The authors acknowledge support of the Russian Foundation of Basic Research (grants Nos 13-02-00627 and 13-02-97131) and the Russian Federation Government contract No 14.B25.31.0015 for Leading Scientists to Russian Educational Institutions. Matveev L.A. acknowledges support of grant No MK-4826.2013.2 of the President of the Russian Federation.

REFERENCES

[1] Schmitt, J., “OCT elastography: imaging microscopic deformation and strain of tissue,” Optics express 3, 199211 (1998).
[2] Sun, C., Standish, B., and Yang, V. X. D., “Optical coherence elastography: current status and future applications,” Journal of Biomedical Optics 16, 043001 (2011).
[3] Kennedy, B.F., Kennedy, K.M., Sampson, D.D., "A Review of Optical Coherence Elastography: Fundamentals, Techniques and Prospects," IEEE Journal of Selected Topics in Quantum Electronics 20(2), 1-17 (2014).
[4] Rogowska, J., Patel, N. A., Fujimoto, J. G., and Brezinski, M. E., “Optical coherence tomographic elastography technique for measuring deformation and strain of atherosclerotic tissues,” Heart 90, 556562 (2004).
[5] Rogowska, J., Patel, N., Plummer, S., and Brezinski, M. E., “Quantitative optical coherence tomographic elastography: method for assessing arterial mechanical properties,” The British journal of radiology 79, 70711 (2006).
[6] Sun, C., Standish, B., Vuong, B., Wen, X. Y., and Yang, V., "Digital image correlation–based optical coherence elastography," Journal of biomedical optics 18(12), 121515 (2013).
[7] Fu, J., Pierron, F., and Ruiz, P. D., "Elastic stiffness characterization using three-dimensional full-field deformation obtained with optical coherence tomography and digital volume correlation," Journal of biomedical optics 18(12), 121512 (2013).
[8] Nahas, A., Bauer, M., Roux, S., and Boccara, A. C., "3D static elastography at the micrometer scale using Full Field OCT," Biomedical Optics Express 4, 2138-2149 (2013).
[9] Hild, F., and Roux, S., “Digital image correlation: from displacement measurement to identification of elastic properties - a review,” Strain 42, 69-80 (2006).
[10] Evans, S. L., and Holt, C. A., “Measuring the mechanical properties of human skin in vivo using digital image correlation and finite element modeling,” The Journal of Strain Analysis for Engineering Design 44(5), 337-345 (2009).
[11] Pan, B., “Recent progress in digital image correlation,” Experimental Mechanics 51, 1223-1235 (2011).
[12] Wang, R. K., Kirkpatrick, S., and Hinds, M. “Phase-sensitive optical coherence elastography for mapping tissue microstrains in real time,” Applied Physics Letters 90(16), 164105 (2007).

[13] Kirkpatrick, S. J., Wang, R. K., and Duncan, D. D., "OCT-based elastography for large and small deformations," Optics express 14, 1158597 (2006).
[14] Nguyen, T. M., Song, S., Arnal, B., Wong, E. Y., Huang, Z., Wang, R. K., and O'Donnell, M., "Shear wave pulse compression for dynamic elastography using phase-sensitive optical coherence tomography," Journal of biomedical optics 19(1), 016013 (2014).
[15] Adie, S. G., Liang, X., Kennedy, B. F., John, R., Sampson, D. D., and Boppart, S. A., "Spectroscopic optical coherence elastography," Optics express 18, 2551934 (2010).
[16] Kennedy, B. F., Liang, X., Adie, S. G., Gerstmann, D. K., Quirk, B. C., Boppart, S. A., and Sampson, D. D., "In vivo three-dimensional optical coherence elastography," Optics Express 19, 66236634 (2011).
[17] Wang, S., Larin, K. V., Li, J., Vantipalli, S., Manapuram, R. K., Aglyamov, S., Emelianov S., and Twa, M. D., "A focused air-pulse system for optical-coherence-tomography-based measurements of tissue elasticity," Laser Physics Letters 10(7), 075605 (2013).
[18] Kennedy, K. M., Ford, C., Kennedy, B. F., Bush, M. B., & Sampson, D. D., "Analysis of mechanical contrast in optical coherence elastography," Journal of biomedical optics 18(12), 121508 (2013).
[19] Kennedy, K. M., McLaughlin, R. A., Kennedy, B. F., Tien, A., Latham, B., Saunders, C. M., and Sampson, D. D., "Needle optical coherence elastography for the measurement of microscale mechanical contrast deep within human breast tissues," Journal of biomedical optics 18(12), 121510 (2013).
[20] Nahas, A., Tanter, M., Nguyen, T. M., Chassot, J. M., Fink, M., and Boccara, A. C., "From supersonic shear wave imaging to full-field optical coherence shear wave elastography," Journal of biomedical optics 18(12), 121514 (2013).
[21] Li, J., Wang, S., Manapuram, R. K., Singh, M., Menodiado, F. M., Aglyamov, S., Emelianov S., and Larin, K. V. "Dynamic optical coherence tomography measurements of elastic wave propagation in tissue-mimicking phantoms and mouse cornea in vivo," Journal of biomedical optics 18(12), 121503 (2013).
[22] Song, S., Huang, Z., Nguyen, T. M., Wong, E. Y., Arnal, B., O'Donnell, M., and Wang, R. K., "Shear modulus imaging by direct visualization of propagating shear waves with phase-sensitive optical coherence tomography," Journal of biomedical optics 18(12), 121509 (2013).
[23] Matveev, L. A., Zaitsev, V. Yu., Matveyev, A. L., Gelikonov, G. V., and Gelikonov, V. M., "Correlation-stability approach in optical microelastography of tissues," Proceedings of SPIE 8699, 869904 (2013).
[24] Zaitsev, V. Yu., Matveev, L. A., Gelikonov, G. V., Matveyev, A. L., and Gelikonov, V. M., "A correlation-stability approach to elasticity mapping in optical coherence tomography," Laser Physics Letters 10(6), 065601 (2013).
[25] Zaitsev, V. Yu., Matveev, L. A., Matveyev, A. L., Gelikonov, G. V., and Gelikonov, V. M., "Correlation-stability elastography in OCT: algorithm and in vivo demonstrations," Proceedings of SPIE 8802, 880208 (2013).
[26] Zaitsev, V. Yu., Matveev, L. A., Matveyev, A. L., Gelikonov, G. V., and Gelikonov, V. M., "Elastographic mapping in optical coherence tomography using an unconventional approach based on correlation stability," Journal of Biomedical Optics 19(2), 021107 (2014).
[27] Enfield, J., Jonathan, E., and Leahy, M., "In vivo imaging of the microcirculation of the volar forearm using correlation mapping optical coherence tomography (cmOCT)," Biomed. Opt. Express 2, 1184-1193 (2011).
[28] Jonathan, E., Enfield, J., and Leahy, M. J. "Correlation mapping method for generating microcirculation morphology from optical coherence tomography (OCT) intensity images," Journal of Biophotonics 4(9), 583–587 (2011).
[29] Matveev, L. A., Zaitsev, V. Yu., Matveyev, A. L., Gelikonov, G. V., and Gelikonov, V. M., "To the problem of stiffness-contrast quantification in the correlation-stability approach to OCT elastography," Proceedings of SPIE 9031, 903102 (2014).
[30] Mariampillai, A., Standish, B. A., Moriyama, E. H., Khurana, M., Munce, N. R., Leung, M. K. K., Jiang, J., Cable, A., Wilson, B. C., Vitkin, I.A., and Yang, Y. X. D., "Speckle variance detection of microvasculature using swept-source optical coherence tomography," Optics Letters 33, 1530 (2008).
[31] Mariampillai, A., Leung, M. K. K., Jarvi, M., Standish, B. A., Lee, K. K. C., Wilson, B. C., Vitkin, I. A., and Yang, Y. X. D., "Optimized speckle variance OCT imaging of microvasculature," Optics Letters 35, 1257 (2010).
[32] Conroy, L., DaCosta, R., and Vitkin, I.A., "Quantifying tissue microvasculature with speckle variance optical coherence tomography," Optics Letters 37, 3180 (2012).

[33] Lee, K. K., Mariampillai, A., Yu, J. X., Cadotte, D. W., Wilson, B. C., Standish, B. A., and Yang, V. X., "Real-time speckle variance swept-source optical coherence tomography using a graphics processing unit," Biomedical optics express 3(7), 1557 (2012).
[34] Ullah, H., Davoudi, B., Mariampillai, A., Hussain, G., Ikram, M., and Vitkin, I. A., "Quantification of glucose levels in flowing blood using M-mode swept source optical coherence tomography," Laser Physics 22(4), 797 (2012).
[35] Davoudi, B., Morrison, M., Bizheva, K., Yang, Y. X. D., Dinniwell, R., Levin, W., Vitkin, I. A., "A novel optical coherence tomography platform for microvascular imaging and quantification: initial experience in late radiation toxicity patients," Journal of Biomedical Optics 18(7), 076008 (2013).
[36] Sudheendran, N., Syed, S. H., Dickinson, M. E., Larina, I. V., and Larin, K. V., "Speckle variance OCT imaging of the vasculature in live mammalian embryos," Laser Physics Letters 8(3), 247 (2011).
[37] Zaitsev, V. Yu., Gelikonov, V. M., Matveev, L. A., Gelikonov, G.V., Matveyev, A.L., and Vitkin, I.A., "Combining several image-modalities in optical coherence tomography: review of recent trends," Radiophysics and Quantum Electronics, (in print), (2014).
[38] Zaitsev, V. Yu., Matveev, L. A., Gelikonov, G. V., Matveyev, A. L., and Gelikonov, V. M., "Towards free-hand implementation of OCT elastography: displacement-based approaches versus correlation-stability ones," Proceedings of SPIE 9129, 912913 (2014).